Biofunctionalization of 3D-printed silicone implants with immunomodulatory hydrogels for controlling the innate immune response: an in vivo model of tracheal defect repair

J. Barthes, P. Lagarrigue, V. Riabov, G. Lutzweiler, J. Kirsch, C. Muller, E.-J. Courtial, Christophe Marquette, F. Projetti, J. Kzhyskowska, et al.

Biofunctionalization of 3D printed silicone implants with immunomodulatory hydrogels for controlling innate immune response: an in vivo model of tracheal defect repair

J. Barthes[1 #], P. Lagarrigue[1, #], V. Ryabov[3], G. Lutzweiler[1], J. Michel[3] C. Muller[1], E.-J. Courtial[4], C. Marquette[4], F. Projetti[5], J. Kzhyskowska[3], P. Lavalle[1], N.E. Vrana[1,2], A. Dupret-Bories[6]

[1] Institut national de la Santé et de la Recherche Médicale, INSERM UMR1121 "Biomaterials and Bioengineering", 11 Rue Humann, 67085 Strasbourg, France.

[2] Spartha Medical, 14B rue de la Canardière, 67100 Strasbourg, France.

[3] Institute for Transfusion Medicine and Immunology, Medical, Faculty Mannheim, University of Heidelberg, Theodor-Kutzer Ufer 1-3, 68167 Mannheim, Germany.

[4] 3d.FAB, Univ Lyon, Université Lyon1, CNRS, INSA, CPE-Lyon, ICBMS, UMR 5246, 43, Bd du 11 novembre 1918, 69622 Villeurbanne cedex, France

[5] Department of Pathology, Toulouse University Hospital, 1, rue Irene-Joliot-Curie, 31100 Toulouse, France.

[6] Institut Claudius Regaud, Institut Universitaire du Cancer Toulouse Oncopole, 31009 Toulouse France.

# These authors contribute equally

* Corresponding authors :

Dr Julien Barthes : jbarthes25@gmail.com

Dr Agnès Dupret-Bories : Dupret-Bories.Agnes@iuct-oncopole.fr

Abstract

The advances in 3D printed silicone (PDMS: Polydimethylsiloxane) implants provide an outlook for personalized implants with highly accurate anatomical conformity. However, a potential adverse effects such as granuloma formation due to immune reactions still exists. One potential way of overcoming this problem is the control of implant/host interface using immunomodulatory coatings. In this study, a new cytokine cocktail composed of interleukin 10 and prostaglandin-E2 was designed to decrease the adverse immune reaction and promote tissue integration by fixing macrophage into M2 pro-healing phenotype for a long term. *In vitro*, the cytokine cocktail was able to keep the secretion of pro-inflammatory cytokines (TNF-α and IL-6) at a low level and induced the secretion of IL-10 and the upregulation of stabilin-1 (endocytotic scavenger receptor expressed by M2 macrophage). This cocktail was then loaded in a gelatin based hydrogel to develop an immunomodulatory material that can be used as a coating of a medical device. The efficacy of this coating was demonstrated in an *in vivo* rat model during reconstruction of a tracheal defect by 3D printed silicone implants. The coating was stable on silicone implants over 2 weeks and the controlled release of cocktail components was achieved for at least 14 days. *In vivo*, only 33% of the animals with bare silicone implant survived whereas 100% survived with the implant equipped with the immunomodulatory hydrogel. The presence of the hydrogel and the cytokine cocktail diminished the thickness of the inflammatory tissue, the intensity of both acute and chronic inflammation, overall fibroblastic reaction, oedema presence and fibrinoid formation (assessed by histology) and lead to a 100% survival rate. At systemic level, the presence of immunomodulatory hydrogel

decreased significantly pro-inflammatory cytokines like TNF-α, IFN-γ, CXCL1 and MCP-1 levels at day 7 and IL-1α, IL-1β, CXCL1 and MCP-1 levels at day 21. The ability of this new immunomodulatory hydrogel to control the level of inflammation once applied on a 3D printed silicone implant has been demonstrated. Such thin coatings can be applied to any implants or scaffolds used in tissue engineering to diminish the initial immune response, improve integration and functionality of these materials and finally decrease potential complications related to their presence.

Keywords: Immunomodulation, 3d printing, implant, hydrogel, cytokine release, immune response, macrophage

I) Introduction

The use of biomaterials is indispensable in many cases where the reconstruction of an organ is required. For example, in order to repair tracheal defects resulting from cancer, trauma, stenosis or congenital problems, primary end-to-end anastomosis can be used for reconstruction after circumferential resection (if the resection is less than 5 cm in length). However, complications occur in ~20% of patients [1] and this procedure is rarely used for larger tracheal defect [2] where the use of artificial patches is more common for reconstruction [3, 4]. Autologous tissue grafts, such as costal cartilage or pericardium have been used for partial replacement, however, those grafts are difficult to design, induce donor site morbidity and generally do not have proper biomechanical properties [5-7]. Synthetic prostheses such as silicone (also called PDMS: Polydimethylsiloxane), PTFE (polytetrafluoroethylene), PU (polyurethane), or PCL (polycaprolactone) have been used for tracheal reconstructive surgery [8-14]. Nevertheless, the use of these prostheses presents limitations and may be subject to chronic inflammation, infections and in some instances can lead to implant rejection [15-17]. The issues observed in tracheal defect reconstruction are manifestations of a more general problem of adverse immune reactions to biomaterials. The implantation of biomaterials in the body is well known to often trigger adverse immune reactions that can eventually lead to their complete isolation via a process called “Foreign Body Response” (FBR) [18]. If this reaction is not controlled,

the ongoing excessive, chronic inflammation can cause collateral damages to the surrounding tissues, pose potential problems to the systemic homeostasis and lead to major interferences with the healing process around the implanted biomaterial. In the later stages, this will lead to the formation of a fibrous capsule and in some cases benign granulomas resulting in implant impairment/failure [19, 20]. For example, in the aforementioned rate of complications in tracheal resection and reconstruction surgeries, the formation of granulation tissue due to excessive immune reactions comprises a significant portion [1]. The intensity and the extent of the reaction depend on the nature of the material (biodegradable, non-biodegradable, synthetic, natural, etc.), whether it is recognized by the innate and adaptive immune system as a potential threat. Moreover, the processing of the material has significant effects. For example, natural materials such as collagen crosslinked with methods that introduce covalent links is not easily degradable by the immune cells and the enzymatic products released tend to induce more severe immune reactions with the activation of multinucleated giant cells [21].

One of the potential therapeutic targets to overcome this problem is the modulation of innate immune response to biomaterials [22, 23]. In this context, macrophages are one of the main actors involved in the initial reaction to implanted materials. Two properties of macrophages make them a suitable target. Firstly, macrophages are highly plastic cells which respond to different biophysical and biochemical stimuli in their immediate environment, thus the presence of anti-inflammatory signals can induce an anti-inflammatory polarization of macrophages [20, 24]. At this point, the second benefit of targeting macrophages will come into play, as macrophages are known to recruit not only other immune cells, but also vascular endothelial cells and connective tissue cells in the vicinity of the implant [25, 26]. Thus, by providing an anti-inflammatory local microenvironment around implants, a cascade of events is induced with the communication between innate immune cells and the other cell types. By modulating the initial innate immune response in the immediate vicinity of an implant, the long-term outcomes of the immune response to the implant should be improved.

Such immunomodulation around implants can be accomplished through different strategies by i) tuning material physico-chemical properties at the host-biomaterial interface (surface topography, roughness, hydrophilicity, chemical moities) or ii) releasing anti-inflammatory agents directly from the biomaterials [22, 27]. For the former option, control of surface hydrophilicity with oxygen plasma treatment and use of micro patterned structures for controlling macrophage phenotype are some options [28-30]. In the case of delivery of anti-inflammatory agents from implants, Vascencelos et al. demonstrated in an *in vivo* model that the presence of anti-inflammatory resolvin D1 in chitosan foams induced more M2 macrophages (anti-inflammatory phenotype) presence with significant decreases in pro-inflammatory cytokine release [31]. With this second strategy, anti-inflammatory cytokines such as interleukins-4 and -10 (IL-4,IL-10) can be used to polarize innate immune cells around the implants into an anti-inflammatory phenotype and thus promoting tissue regeneration, limiting inflammation and preventing implant failure [32]. However, as macrophages are highly plastic, a crucial objective is to develop cytokine cocktails that can fix the innate immune cell phenotype for a long term. Previously, we have developed a M2 macrophage phenotype fixing cytokine cocktail which was able to induce M2 polarization and facilitate wound healing by fibroblasts *in vitro* [33]. However the *in vivo* effect of such cocktail has not been assessed yet. Moreover, even though we have shown in vitro that conversion of the phenotype of macrophages into M2 state was stable for 6 days after withdrawal of M2 inducing cocktail from culture medium, macrophages could quickly be re-polarized into M1 phenotype upon IFN-γ stimulation. Hence, it is necessary that such cocktails could be released in a controlled manner to sustain anti-inflammatory milieu in the local microenvironment of implanted materials for extended time period.

To modulate host inflammatory response and develop immunomodulatory biomaterials, we can distinguish two different paths. The first option is to modify directly the physico-chemical properties of the implant which might not be feasible in every cases, or the second option is to develop immunomodulatory coatings that will be applied at the surface of the implant. The second option offers a broad range of possibilities to develop a better interface between the implants and the

surrounding tissues. ECM based materials such as hydrogels made of gelatin, collagen, hyaluronic acid due to their biocompatibility properties and easy tunable physical properties have been used for a long time in tissue engineering and regenerative medicine [34]. They can act as delivery systems and also promote tissue regeneration around the implant due to their intrinsic properties (biomechanical, biochemical) that will improve cell adhesion and proliferation [35, 36]. Moreover, due to their natural hydrated state, they are finally good candidates as delivery systems for anti-inflammatory cytokines.

In the past few years, we have been working on the development of ECM based surface coatings to modulate cell behavior in either 2D or 3D microenvironment [37-39] . We have shown that bioactive molecules such as IL-4 can be successfully loaded and release from these ECM based coatings and a significant change in macrophage behavior can be induced [40].

In this current study, we aim to demonstrate the efficacy of such immunomodulatory coatings *in vivo* at the surface of an implant using a commonly used non-degradable biomaterial in 3D printed format, silicone. Such silicone implants are commonly used in major clinical pathology, like tracheal defects following cancer surgeries or traumas that both require most of the time tracheal regeneration with a biomaterial (tracheal defect model).

Silicone is regularly used in head and neck reconstruction surgery because of its biocompatibility [41-43] and thanks to the latest advance in 3D printing methods, silicone materials may be currently 3D printed to develop personalized implant with a perfect anatomical fit [11-13, 44, 45]. However, silicone has been widely reported to induce excessive inflammation, granuloma formation and crusting [46, 47] so it is a “ideal” material to study the adverse immune reactions

In order to demonstrate *in vivo* the efficacy of an immunomodulatory hydrogel containing a phenotype controlling cytokine cocktail, a 3D printed silicone tracheal patch was used as a model implant. Gelatin hydrogel enzymatically crosslinked with microbial transglutaminase was used as the surface coating The immunomodulatory hydrogel has been applied to the implant surface with the aim to limit excessive inflammation after implantation. The coating has been loaded with a pro-

healing and anti-inflammatory cytokines cocktail (called “M2Ct2”) to develop immunomodulatory hydrogel. This M2 inducing cocktail was optimized to reduce the expression of major metalloproteinases MMP7 and MMP9 [33] involved in gelatin degradation to avoid fast degradation of the hydrogel. After demonstration of the coating stability on implants, we carried out an *in vivo* study on male Wistar rats to demonstrate the beneficial effect of the immunomodulatory coating to repair a partial tracheal defect equivalent.

2) Materials and methods

2.1. Materials

Gelatin Type A from porcine skin (Mw = 5-10 x 10^4 Da), fluorescein isothiocyanate-labeled bovine albumin (BSA^{FITC}, Mw = 6.6 x 10^4 Da) were purchased from Sigma-Aldrich (St Quentin Fallavier, France). Dulbecco’s Phosphate buffered saline was obtained from Life Technologies (Carlsbad, USA). Microbial transglutaminase (mTG, Mw = 3.8 x 10^4 Da) was kindly provided by Ajinomoto Inc (Tokyo, Japan). IL-10 (human, recombinant) (Mw = 1,86 x 10^4 Da), IL-10 (rat, recombinant) (Mw = 1,86 x 10^4 Da) and Prostaglandin-E2 (Mw = 3.52 x 10^2 Da) were purchased from Promokine (Heidelberg, Germany). Rat inflammation panel (13-plex) with V-bottom plate was purchased from Biolegend. Fluorescein isothiocyanate-labeled gelatin ($Gelatin^{FITC}$) from porcine skin was purchased from ThermoFisher Scientific. Ketamine (Ketamine 500®, VIRBAC), Xylazine (Rompun®) Buprenorphine (Buprecare®), Pentobarbital (Penthotal®), Isoflurane (1.5-2.0%) were obtained from Centravet (Nancy, France).

Silbione® LSR 4350 from Elkem Silicones was used as a model of silicone bi-components formulation. Parts A and B components of LSR are designed to be mixed in equal parts (1:1) at room temperature. The classical part B with high concentration of inhibitor agent was used in order to keep a high pot-life (>24h) after mixing. This data is important in order to keep the same rheological behavior of LSR throughout 3D printing. Polyethylene Glycol 400 (Sigma-Aldrich, USA) were used as yield stress agents. The addition of Polyethylene Glycol 400 in LSR was performed in part A at 2% mass fraction

of part A. Then, part B was added to part A in a 1:1 (w/w) ratio at room temperature. After mixing, samples were included in 10 cc single cartridges (Nordson® EFD, USA) and degassed through centrifugation at 4000 rpm for 5 minutes (Eppendorf 5810R, Germany). After printing, the LSR structures were thermal cured in a two-step protocol: room temperature for 72h and 175°C for 120 minutes.

2.2. Cell culture experiments and immunostaining

2.2.1. Isolation of human monocyte-derived macrophages and cytokine stimulations

Monocytes were isolated from buffy coats of healthy donors as described previously [33, 48]. Monocytes were cultured at 1×10^6 cell.mL^{-1} in serum free macrophage-SFM medium (ThermoFisher Scientific) supplemented with 10 ng.mL^{-1} M-CSF (Peprotech), 10^{-8} M dexamethasone (Sigma-Aldrich, Munich, Germany), M2Ct1 consisting of IL4 (3 ng.mL^{-1}) + IL10 (10 ng.mL^{-1}) + TGFβ1 (10 ng/mL) or M2Ct2 consisting of IL10 (10 ng.mL^{-1}) + prostaglandin E2 (20 ng.mL^{-1}) for 6 days. All cytokines were purchased from Peprotech. LPS (Invivogen) was added to the cells in concentration of 1 µg.mL^{-1} for 24 h.

2.2.2. Elisa

The concentrations of TNF-α, IL6, MMP7, and MMP9 were measured in macrophage cell culture supernatants using human DuoSet ELISA kits (R&D Systems) according to manufacturer instructions.

2.2.3. RT-qPCR

Expressions of stabilin-1 and IL-10 under different stimulations were compared using predesigned TaqMan assays for stabilin-1 (Hs 01109068) and IL-10 (Hs 00961622) (ThermoFisher Scientific). Normalization of gene expression levels was performed using housekeeping gene GAPDH.

2.2.4. Cells encapsulation in gelatin hydrogel

Monocytes were isolated as described in 2.2.1. Cell encapsulation was carried out as described before [49]. After isolation, monocytes were centrifuged and then gelatin solution was added at 37°C

on cells pellets in order to get a cell density of $6x10^6$cells.mL^{-1} of gelatin. Finally, mTG and gelatin solution were mixed together in a volume ratio of 5/1 in order to get a final concentration of gelatin hydrogel of 6% (w/v). 200 µL of gelatin hydrogel were deposited in 12 well-plate and let crosslinked for 30 min at 37°C before the addition of cell culture medium (SFM medium) supplemented with either M2Ct2 cocktail (IL-10: 10 ng.mL^{-1} + prostaglandin-E2: 20 ng.mL^{-1}), IL-4 (10 ng.mL^{-1}) or no supplementation NS) and the cell-laden hydrogels were cultured for 12 days. Medium were changed every three days.

2.2.5. Immunostaining (RS1 and CD68)

At different time of monocyte encapsulation experiment, cells were fixed with paraformaldehyde (3.7% v/v) in PBS. CD68 was stained with mouse anti-human CD68 (MSKO55-5, Zytomed, Berlin, Germany) at a dilution 1:100 followed by the appropriate labeled secondary antibody, donkey anti-mouse Alexa 647 (725-607-003, Dianova, Hamburg, Germany) at a dilution of 1:400). Stabilin-1 was stained with custom-made rabbit human RS-1 (PSL, GmbH; Heidelberg, Germany) at a dilution of 1:400 followed by the appropriate secondary antibody, donkey anti-rabbit Cy3 (711-165-152, Dianova) at a dilution of 1:400 as previously described [50]. Nucleus were stained with DAPI (236276, Roche, Basel, Switzerland) at a dilution of 1:1000. Samples were then analyzed with confocal microscope (ZEIS LSM 710).

2.3. Tracheal patches elaboration

2.3.1. Gelatin and microbial Transglutaminase (mTG) solutions

Gelatin solution used to prepare hydrogel coating was prepared at 6 % (w/v) from gelatin type A in PBS supplemented with 1% (v/v) penicillin/streptomycin and 0.2% (v/v) fungizone. PBS solution was added to the Gelatin type A powder under biosafety cabinet to keep the solution sterile. The solution was heated at 50°C for 30 minutes under stirring. Then the solution was filtered with 0.22µm syringe filters. Microbial Transglutaminase (mTG) solution used to crosslink the hydrogel was prepared at

20% (w/v) from transglutaminase powder (Ajinomoto, Activa, 86-135 units.g^{-1}) in PBS with Pen/Strep and fungizone. The addition of PBS solution is performed under biosafety cabinet.

For stability test, gelatin solution labelled with fluorescein isothiocyanate (FITC, Molecular probes by Life Technologies) was prepared. The same protocol as described before to prepare a 20mL gelatin solution was used and then 5mg of gelatin type A FITC was added to the mixture.

2.3.2. 3D printing of Tracheal patches

Silicone tracheal patches were 3D-printed using the liquid deposition manufacturing technique through COSMED cartesian 333 3D printer (Tobeca, France)[45]. The movement precision of this printer is 10 µm. Silicone formulation were contained in 10 cc cartridges equipped with standard piston and 400 µm diameter conical nozzle (Nordson EFD, USA). The 3D printing was controlled with Repetier Host software (Repetier, V2.0.1, Germany). Dispensing flow rate was controlled by an Ultimus V pneumatic equipment (Nordson EFD, USA) using HP10cc system. Slicing of 3D objects was performed with Slic3r software (Slic3r, V3, Italia) using appropriated spiral printing parameters.

The implants were designed as cylindrical structures corresponding to the size and shape of two rings of healthy rat trachea. Tracheal patches dimensions are based on rat's natural trachea and have the following dimensions: Inner diameter = 3 mm, Height = 5 mm and Wall thickness = 0.7 mm.

The implants were cleaned in ultrasonic bath for 5 minutes in ethanol and then for 5 minutes in deionized water. O_2 plasma cleaner treatment was then performed for 1 min to increase silicone wettability. The plasma cleaner treatment must be done just before gelatin deposition.

2.3.3. Hydrogel coating

To deposit the gelatin hydrogel on the outer surface of our implants, a special holder was developed (Figure 6) to perform the impregnation of the implants in the gelatin solution 6% (w/v). Gelatin solution must be kept at 50°C before impregnation. Once the silicone tube implants are placed on the holder, they were fully immersed it in the gelatin solution for 30 minutes. Then the implants were placed in dry condition on the holder for 2 hours at room temperature. If the implants are not immediately crosslinked, they must be kept at 4°C. To crosslink the hydrogel, holder containing

implants was immersed in mTG solution 20% (w/v) at room temperature for 6 hours and let dry for 2 hours at room temperature. The implants were kept at 4°C and were sterilized 15 min under U.V. light before use.

2.3.4. Loading of bioactive molecules in the hydrogel

The hydrogel coated implants were loaded with different bioactive molecules. First, release tests were performed with BSA^{FITC}, a model molecule commonly used in preliminary release tests. BSA^{FITC} solution at 1mg/mL was prepared and implants were immersed in 1mL bath. After 12 hours incubation at 4°C, samples were kept dry under safety cabinet 1 hour before starting release tests.

To test the release of M2Ct2 cocktail, IL-10 and PGE-2 were loaded in the hydrogel and released in PBS solution. In our previous studies [33], it was shown that the cocktail needed to be concentrated at least 10 times once loaded in a hydrogel *in vitro* under static conditions. So, as *in vivo* the potential of cytokine loss was higher due to the presence of physiological flows, for this study we have decided to multiply the concentration of M2Ct2 (initially 10 ng/mL IL-10 and 20 ng/mL PGE-2) by a factor 50 so respectively 500 ng/mL IL-10 and 1 µg/mL PGE-2. In order to load these biomolecules, 1mL of either IL-10 or PGE-2 prepared in MilliQ water (18,2 MΩcm, Millipore) at respectively 500 ng/mL or 1µg/mL were incubated on the coated tracheal patches for 12 hours at 4°C. Then the samples were kept dry 1 hour under safety cabinet before performing the release test.

2.4. Implant characterization

2.4.1. Hydrogel stability

Two different tests were performed to check gelatin hydrogel stability on silicone implants. Tests were performed for 14 days, the samples were incubated in 1mL of culture medium without serum and supplemented with 1% (v/v) penicillin/streptomycin and 0.2% (v/v) fungizone at 37°C and then read outs were performed at days 0, 7 and 14.

2.4.1.1. Sirius red/fast green test

In order to evaluate the hydrogel coating stability, “Sirius Red/Fast Green collagen staining kit” provided by Chondrex was used. This test allows the determination of the amount of collagen and non-collagenous proteins which gives an indirect quantification of gelatin at the surface of the implant. The protocol was carried out as described in the kit. Samples were firstly rinsed with PBS two times, then samples were immersed in dye solution for 30 min. Afterwards, the samples were rinsed with distilled water several times until the water became clear. Samples were then immersed in 1 mL of Dye extraction buffer for 15 min. 100 µL of the solution were collected in a 96-well plate, and absorbance values at 540 and 605 nm were recorded with a spectrophotometer. The collagenous part part was calculated with the equation given in the kit protocol:

$$\text{Collagenous part (µg of protein/ mg of material)} = \frac{(\text{OD } 540 \text{ nm} - (\text{OD } 605 \text{ nm} * 0{,}291)}{0{,}0378 * \text{scaffold weight}}$$

OD 540 nm and OD 605 nm are the optical density at 540 and 605 nm respectively. For each experimental condition, a sample without cells was used as a control.

Moreover, as the red dye will specifically bind to collagen, so to gelatin also, the hydrogels were labeled in red, a visual observation was possible.

2.4.1.2. Gelatin FITC

To evaluate the homogeneity of the hydrogel coating, gelatin^{FITC} was used to cover our implants. The samples were observed with confocal microscope (LSM 710, Zeiss) at day 0, 7 and day 14 and the evolution of coating thickness was followed overtime.

2.4.2. Release tests

Gelatin hydrogel coating implants was loaded with two different biomolecules (BSA and PGE-2) as explained in the part 2.4. Release tests were performed by immersing the samples in 1 mL of PBS (supplemented with Pen/Strep and Fungizone) at 37°C. Regular read outs were performed for 21 days and after each recording supernatant was replaced by fresh PBS medium.

Data from BSA^{FITC} loaded samples were analyzed with a spectrofluorimeter (Xenius, Safas, Monaco). The excitation wavelength was 495 nm and the emission wavelength was 525nm. A cumulative release was then performed and thanks to a calibration the exact mass of BSA released was calculated. IL-10 and PGE-2 release tests were performed with the same protocol; however, the quantification of the release was assessed with ELISA tests (Promokine).

2.4.3 Contact angle measurement

Surface wetting properties of the raw silicone and plasma-treated silicone were determined by contact angle measurement with MilliQ water using the sessile drop technique (Attension theta, Biolin Scientific). The images were analyzed with the software Oneattension.

2.4.4. Surface roughness of 3D printed patch

An ultra-high precision optical profilometer (NanoJura, France) was used to evaluate the roughness profile of patches surface (uncertainty 16 nm on Ra 1 micrometer). Scanning was performed at 500Hz with 1µm/s acquisition speed.

2.5. *In vivo* tests

Twenty-four 8-week-old male Wistar rats (300-400 g in weight), provided by a certified breeding centre (Charles River, BP 0109, F 69592, L'Arbresle, France) were used for this study. The animals were received at the CREFRE (US 006/CREFRE - Inserm/UPS/ENVT) animal supplier (No. A31555010 issued December 17, 2015). Protocols were submitted to the CREFRE ethics committee with approval number DAP-2017010313429985, in accordance with the European directive (DE 86/ 609/CEE; modified DE 2003/65/CE) for conducting animal experiments. One week of acclimatization was respected. The animals were housed in ventilated cages with a double level (two animals per cage according to European standards). The animals were carefully monitored (behavior and food intake) and were weighed weekly throughout the experiment. The 22 rats were divided in three implantation groups to be explanted after 21 days. The first group was implanted with Silicone implant alone (6 rats, control: **PDMS** condition), the second group with hydrogel coated Silicone

implant (8 rats, Gelcondition) and the last group with the immunomodulatory hydrogel coated Silicone implant (8 rats, hydrogel coating loaded with M2Ct2 cocktail: **M2Ct2** condition). To evaluate the inflammatory response after implantations, different analyses were performed to check the fluctuation of the inflammation markers after implantation: in the tissue the inflammation related markers were checked using RT-PCR and histology and at systemic level the inflammation level was quantified by detection of cytokines in the blood by flow cytometry.

2.5.1. *In vivo* implantations

Samples were prepared for the *in vivo* tests using the same protocol explained in part 2.3. A preliminary anesthesia of the animals was performed with an isoflurane gas anesthesia device. Once rats were anesthetized, they were kept under anesthesia thanks to anesthesia mask and an intraperitoneally injected anesthetic solution (Ketamine 90 $mg.kg^{-1}$ and xylazine 10 $mg.kg^{-1}$). Each rat was placed in a supine position on a heated pad. Then rats were shaved and cleaned with betadine around the neck area before proceeding to the vertically incision from the jaw down to the sternum. Subhyoid muscles were separated from the trachea. The implant was cut to create a tracheal patch which matches with rat's trachea shape. Then a window in the trachea was created which corresponds to the removal of two tracheal rings and the implant was placed over the window. The implant was fixed in the trachea with sutures (Figure 1). To finish the operation, muscles and incision were closed with stitches. 0.05 $mg.kg^{-1}$of Buprecare was injected to the animal in subcutaneous route for pain reduction at the end of the implantation and every 12 hours for 5 days. Euthanasia were performed after 21 days or when animal showed respiratory distress symptoms. The animal was first anesthetized with isoflurane device and mask and then slowly injected with an overdose of pentobarbital (150 mg/kg) in intraperitoneal route. After the expiration of the animal, the tracheal patch was explanted, and surrounding tissue was collected to perform histology and PCR analyses.

For cytokines level quantification tests, using flow cytometry, we collected blood sample of each rat at day 7, 14 and 21 under anesthesia with an isoflurane gas anesthesia device. The tail was disinfected and a 23G needle was placed into the vein at 15/20° angle starting approximately one

third from the end of the tail. Blood up to 2 mL was collected with a syringe and directly sent for quantification of pro-inflammatory cytokines. Applying pressure with sterile gauze to achieve hemostasis stopped blood flow.

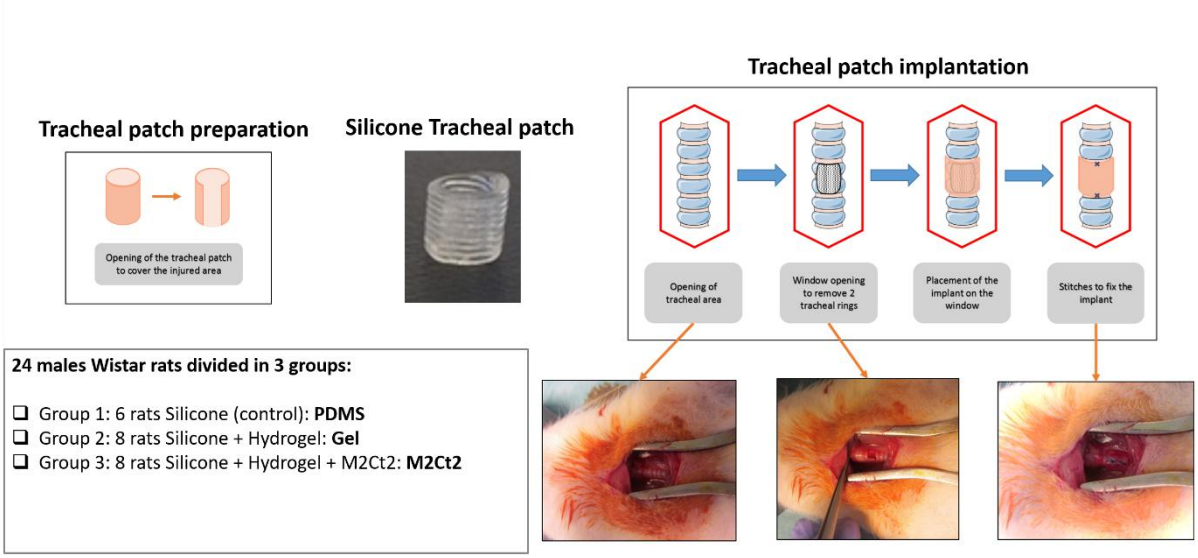

Figure 1. *In vivo* experiment design to repair tracheal defect in a rat model with a 3D printed silicone tracheal patch.

2.5.2. Cytokines cocktail loading

For the third group, the immunomodulatory hydrogel coated implants, gelatin hydrogels were loaded with M2Ct2 cocktail composed of Interleukin 10 (IL-10) and Prostaglandin-E2 (PGE-2) for rats. The sterilized samples were incubated with 1 mL of solution containing 1 $\mu g.mL^{-1}$ of PGE-2 and 500 $ng.mL^{-1}$ of IL-10. Implants were incubated for 12 hours at 4°C. At the end of incubation, the solution was removed, and the samples were kept in dry condition until the implantation.

2.5.3. Histology

Tracheal patches were fixed in 4% formalin. Macroscopic transverse sections were embedded in paraffin. Five-µm thick sections were stained with hematoxylin-eosin-saffron (HES). For each sample, microscopic optical analysis was realized with the software NDP.view2 (Hamamatsu, Massy, France) after slide scanning (NanoZoomer, Hamamatsu) with the following criteria: semi-quantitative assessment of acute inflammation, chronic inflammation, fibroblastic reaction, edema, and periprosthetic histiocytic reaction; assessment of the periprosthetic fibrinoid deposition, and tracheal

ulceration; and measure of the maximal thickness of fibro-inflammatory reaction between implant and trachea.

2.5.4. Quantification of pro-inflammatory cytokines in blood serum with flux cytometry

Blood was collected at different time points and Pro-inflammatory cytokines from blood serum were measured using BioLegend's LEGENDplex™ assay (Rat inflammation Panel (13-plex)) according to manufacturer specifications. Data were acquired on a BD LSRII cytometer and analyzed using LEGENDplex™ Data analysis software.

2.6 Statistical analysis

The statistical significance of the obtained data was assessed using One-way ANOVA with Tukey's multiple comparisons or Friedman test with Dunn's multiple comparisons ($n \geq 3$). The error bars were representative of standard deviation (SD). Differences at $p \geq 0.05$ were considered statistically insignificant.

3) Results and Discussion

3.1 Optimization of the cocktail *in vitro*

Previously, we developed a cytokine cocktail called "M2Ct1" based on IL-4, IL-10 and TGF-beta that was able to maintain M2-like macrophage phenotype much longer than conventional strategies using IL-4 alone [33, 51]. The presence of macrophages differentiated with this cocktail improved fibroblast-mediated wound healing *in vitro*. However, prior to application of such cocktails *in vivo*, their effect on the secretion of major macrophage-produced matrix metalloproteinases (MMP7 and MMP9) needed to be checked. Indeed, MMPs are involved in many inflammatory reactions and contribute to the degradation of extracellular matrix of tissues. Their presence at the implant/host interface would compromise the integration of the implants. MMP7 level needs to stay low since it induces other pro-MMPs secretions resulting in an exponential increase in extracellular matrix

degradation. In patients with peri-implantitis, the level of active MMP-7 and MMP-8 were shown to be significantly increased [52]. In the present study, the cocktail “M2Ct1” was first tested in solution with Human monocyte-derived macrophages to evaluate MMP7 production and it demonstrates that it induces significant amounts of secreted MMP-7 (Figure 2). As high level of MMP-7 is a potential impediment to the integration of the implant, we reformulated our cytokine cocktail and substituted IL-4 and TGF-beta with prostaglandin E2 (PGE2), a potent inhibitor of pro-inflammatory cytokine production in macrophages [53-55]. This new cocktail was called “M2Ct2”. M2Ct2 cocktail was as efficient as initial cytokine cocktail M2Ct1 in terms of inhibition of TNF-α and IL-6 produced by LPS-stimulated macrophages and moreover M2Ct2 was able to prevent induction of MMP-7 release (Figure 2). In addition, M2Ct2 induced higher expression of IL-10 and stabilin-1, both known as M2 macrophage markers as detected by RT-PCR (Figure 2). For both cocktail formulations M2Ct1 and M2Ct2, the secretion of MMP-9 that is another important matrix metalloproteinase in inflammatory tissue degradation, was insignificant. Following these improvements in the cocktail formulation, M2Ct2 was selected for the rest of the study.

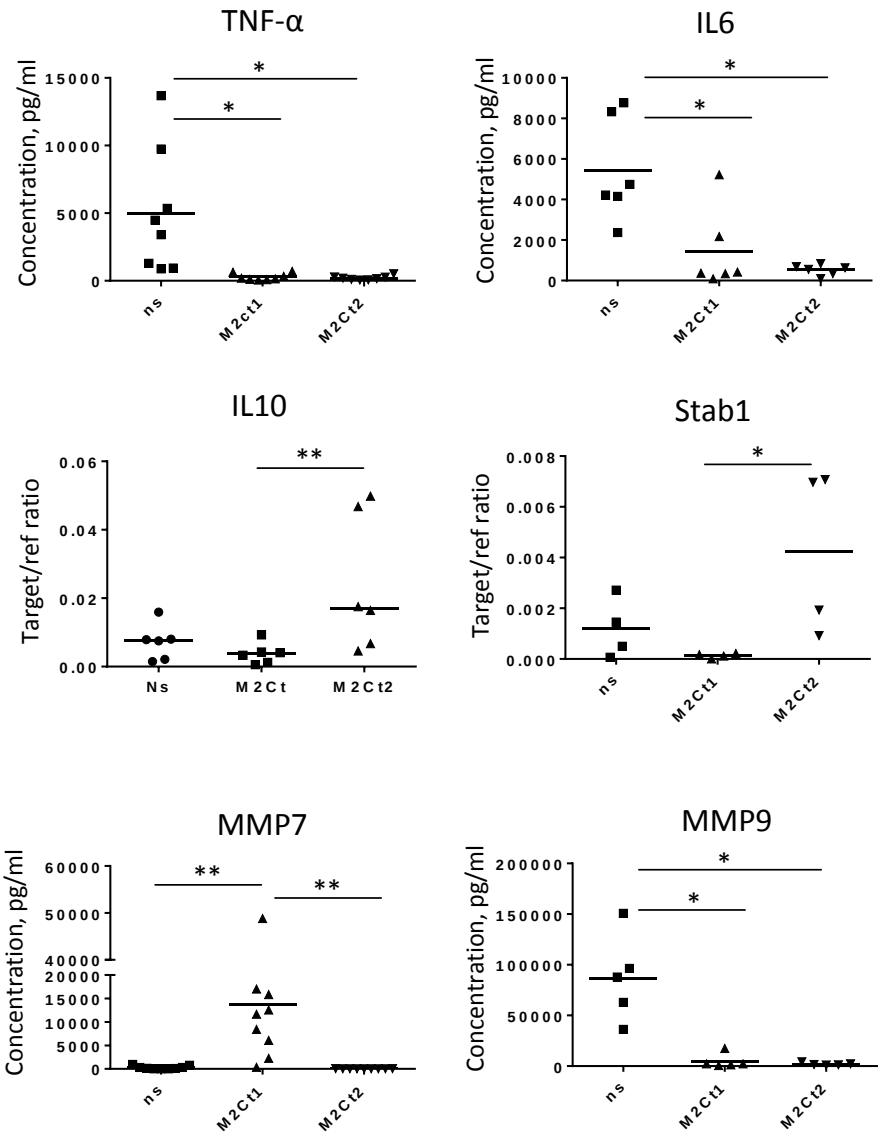

Figure 2: Human monocyte-derived macrophages were isolated from peripheral blood of healthy donors and cultured for 6 days without stimulation (SFM medium) or in cell culture medium (SFM) supplemented with M2Ct1 or M2Ct2. The concentrations of TNF-α, IL6, MMP7 and MMP9 in cell culture supernatants were assessed using ELISA. For the assessment of TNF-α and IL6 release macrophages were stimulated with LPS (1 µg/ml) for 24h. The expression of IL10 and Stab-1 was measured using RT-qPCR on day 6 of culture and normalized with housekeeping gene GAPDH (n=6), *p<0.05, **p<0.01.

3.2 Effect of the M2Ct2 cocktail on monocytes in 3D culture conditions

Even though monocytes will be attracted to the surface of the implant, this will happen in a 3D connective tissue microenvironment. Thus, in order to mimic such environment, we used a 3D culture model where the monocytes are encapsulated in gelatin hydrogels in the presence or absence of the cytokines [40, 56]. In order to see the effect of the new M2Ct2 cocktail, primary monocytes were encapsulated in gelatin hydrogel and then cultured for 12-days in cell culture medium i) without stimulation NS (SFM medium) or supplemented with either ii) IL-4 (10 $ng.mL^{-1}$) or iii) M2Ct2 cocktail (IL-10: 10 $ng.mL^{-1}$ + prostaglandin-E2: 20 $ng.mL^{-1}$). In this experiment, IL-4 was used as a control since it is one the most common inducers of M2 differentiation [20]. After 12 days, we quantified the CD68+ cells and stabilin-1 expression using confocal microscopy (Figures 3 and 4). CD68 is a pan-macrophage marker which can be used to identify the differentiation of the encapsulated monocytes into macrophages. Stabilin-1 is a transmembrane protein involved in endocytosis of bacteria and also of lipids such as malondialdehyde-LDL (MDA-LDL) [57]. It has been shown that stabilin-1 expression by tissue-infiltrating macrophages provide a defense against oxidative collateral tissue damage via decreasing the secretion of CCL3 (a known profibrogenic cytokine) [58]. This contributes to the faster resolution of inflammation thus, the induction of its expression provide a microenvironment with less oxidative stress that could be beneficial in the context of implantable materials.

Figure 3 shows that in 3D culture conditions, the presence of the M2Ct2 cocktail induced significantly higher number of CD68+ macrophages compared to encapsulated naïve monocytes and similar numbers in the presence of IL-4, demonstrating that it has a similar capacity for induction with IL-4 . Moreover, the levels of expression of stabilin-1 were clearly higher in the case of cocktail infused hydrogels after 12 days with similar cellular densities with naïve monocytes and IL-4 supplemented conditions (Figure 4). This 3D culture results demonstrate that the M2Ct2 cocktail retains its ability to influence a pro-regenerative macrophage phenotype in 3D proteinaceous, hydrated microenvironment conditions.

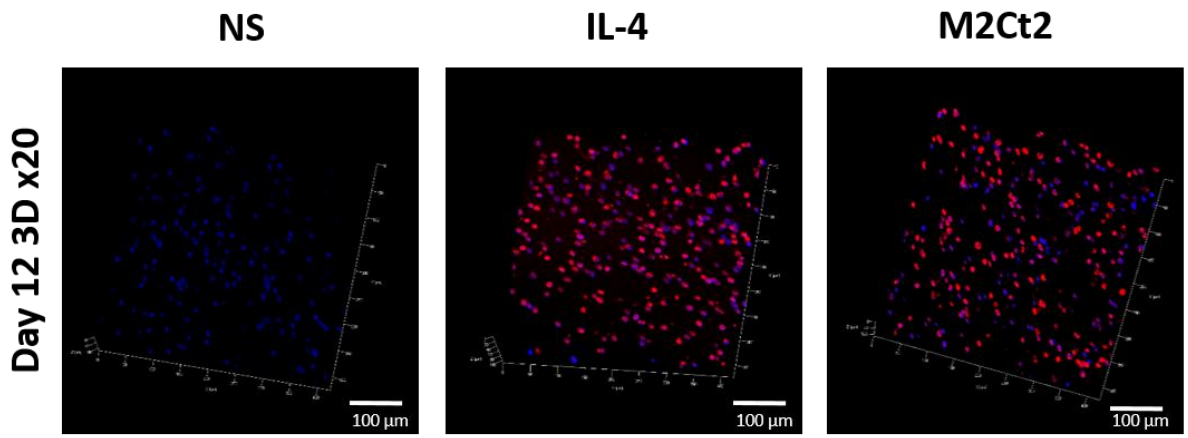

Figure 3: 3D Confocal images at 20x magnification of DAPI (blue) / CD68 (red) stainings with encapsulated naïve monocytes in gelatin hydrogel after 12 days of culture in three different conditions i) medium non-supplemented (NS), ii) supplemented with IL-4 (IL-4) or supplemented with M2Ct2 cocktail (M2Ct2).

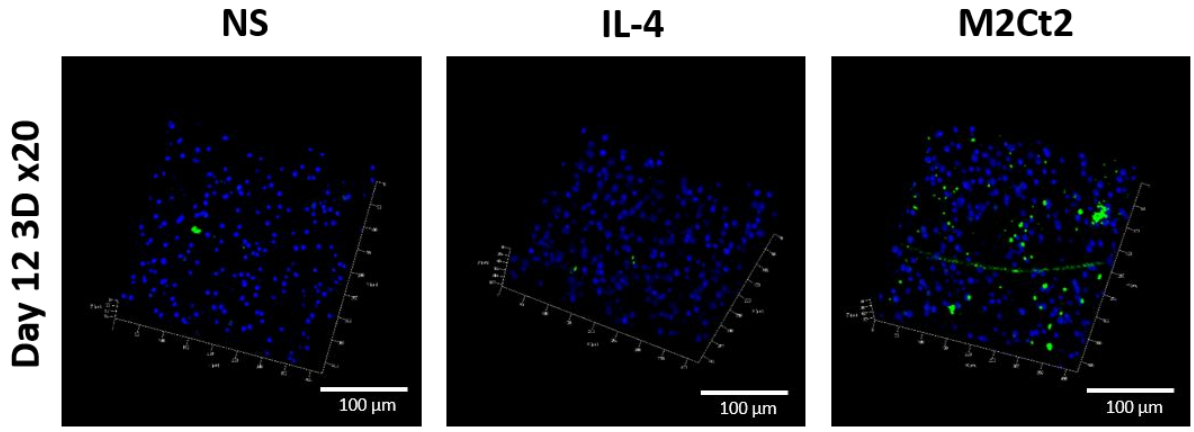

Figure 4. 3D Confocal images at 20x magnification of DAPI (blue) / RS1 (stabilin, green) stainings with encapsulated naïve monocytes in gelatin hydrogel after 12 days of culture in three different conditions i) medium non-supplemented (NS), ii) supplemented with IL-4 (IL-4) or supplemented with M2Ct2 cocktail.

3.3 3d printing of the patch and hydrogel coating

Silicone formulation was printed to manufacture silicone tracheal patches from the STL (Standard Tessellation Language) file (Figure 1) , the dimensions are the following: Inner diameter = 3 mm, Height = 5 mm and Wall thickness = 0.7 mm. After the curing of the patch, gelatin hydrogel was coated on the outer part of the tracheal ring using a specific sample holder and impregnation process was performed as described in Figure 5.

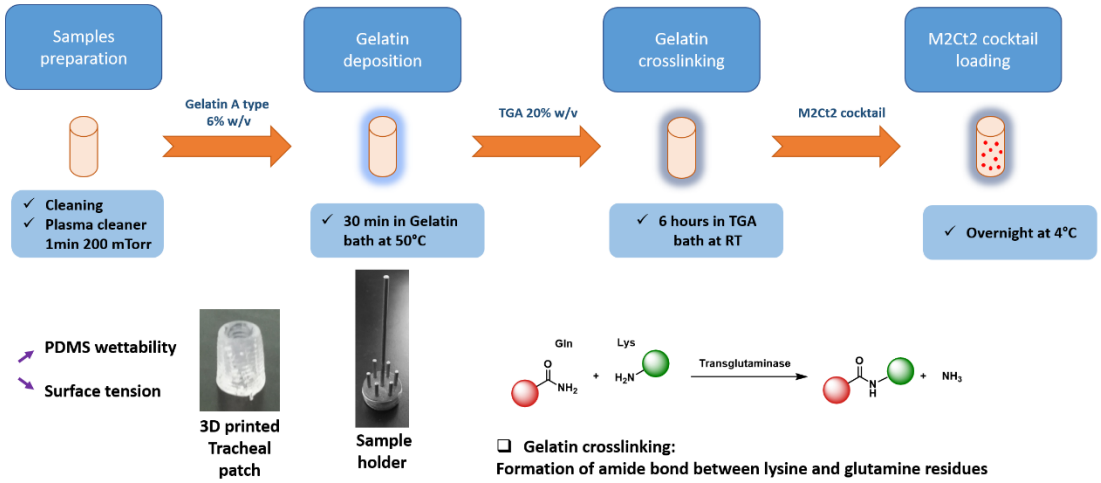

Figure 5: Protocol to coat gelatin hydrogel and load M2Ct2 cocktail on 3D printed silicone tracheal patch.

The final roughness was about 20 µm (Figure S1). To improve silicone implant wettability in order to obtain a more hydrophilic surface and hence to facilitate gelatin deposition, the implant was treated with oxygen plasma cleaner prior to gelatin deposition. The hydrophilicity of the silicone-based implant has increased as shown in Figure S2 with a contact angle decreasing from 108° to 3° after oxygen plasma treatment.

Then after gelatin deposition, the hydrogel was enzymatically crosslinked using microbial transglutaminase mTg to improve its stability. Indeed, transglutaminase catalyzes the formation of amide bond between carboxamide (RCONH2) from glutamine and primary amine moieties from lysine. The stability of the coating at the surface of the implant in cell culture medium at 37°C was

tested using two different techniques. The first technique was based on the quantification of gelatin amount using Sirius Red/Fast Green kit. Samples were immersed in cell culture medium in incubator (37°C, 5% CO_2). We observe that after an initial loss of the coating (about 50%) the first week, the coating remains stable on the implant after 14 days (Figure 6A). The implant was still red after two weeks meaning that gelatin hydrogel was still attached on the surface (Figure 6B). A second technique to check coating stability on silicone tracheal patch was also performed and it was based on the use of fluorescently labeled gelatin (Gelatin-FITC). The thickness of gelatin coating was estimated at different time point of immersion of cell culture medium at 37°C (D0, D7 and D14) using confocal microscope (Figure 6D). After gelatin deposition (D0), the thickness of the coating was estimated around 30 µm (Figure 6C) and then after 1 week of immersion in cell culture medium in incubator (37°C, 5% CO_2), we observed a decrease of the thickness to 15µm suggesting a loss of about 50% of the coating Then the thickness remained stable up to the next measurement at day 14. These two techniques used to estimate coating stability on the silicone tracheal patch gave the same trend. After an initial loss of about 50% of the coating the first week, the coating remained stable at the surface until day 14. With our protocol we were then able to coat gelatin-based hydrogel on silicone implant and thus modifying the interface between the implant and the surrounding environment with an ECM based material.

3.4 Release properties

The next step was to investigate the ability of the surface coating to act as a delivery platform for bioactive molecules. We first investigated the release properties using a model protein, BSA fluorescently labeled (BSA-FITC) and we performed a cumulative release for 2 weeks in PBS at 37°C (Figure S3). After an initial burst release, we observed a steady release of BSA until reaching a plateau after about 2 weeks. Then we quantified the loading and the release of one molecule used in the M2Ct2 cocktail (PGE-2). To ensure an efficient loading and release of the M2Ct2 cocktail *in vivo* from the gelatin hydrogel, we used a concentration 50 times greater than the initial concentration of the cytokines cocktail used previously in in vitro tests. Thus, the tracheal patches were incubated

overnight at 4°C in 1 mL of solution containing 1 µg.mL^{-1} of PGE-2. First the loading efficiency was quantified with Elisa test for PGE-2 by quantifying the remaining mass of PGE-2 in the incubation bath after the loading. A value of about 39% was determined (figure S4). Then release experiments of this molecule was performed *in vitro* in PBS at 37°C (Figure 6E). A burst release was observed the first day with almost 28% of release in the medium of the PGE-2 loaded in the hydrogel and then only few percents are released until day 14. This means that nearly 70% of the molecules initially loaded in the hydrogel was still in the hydrogel after 2 weeks of release so this hydrogel can really act as a reservoir for bioactive molecules. Monocytes in vivo will be mainly in contact with the implant during the first week, so they will be directly impacted and differentiated by the cocktail. Then, a slow release related to hydrogel degradation will occur and will probably release the rest of the cocktail, preventing a strong inflammation.

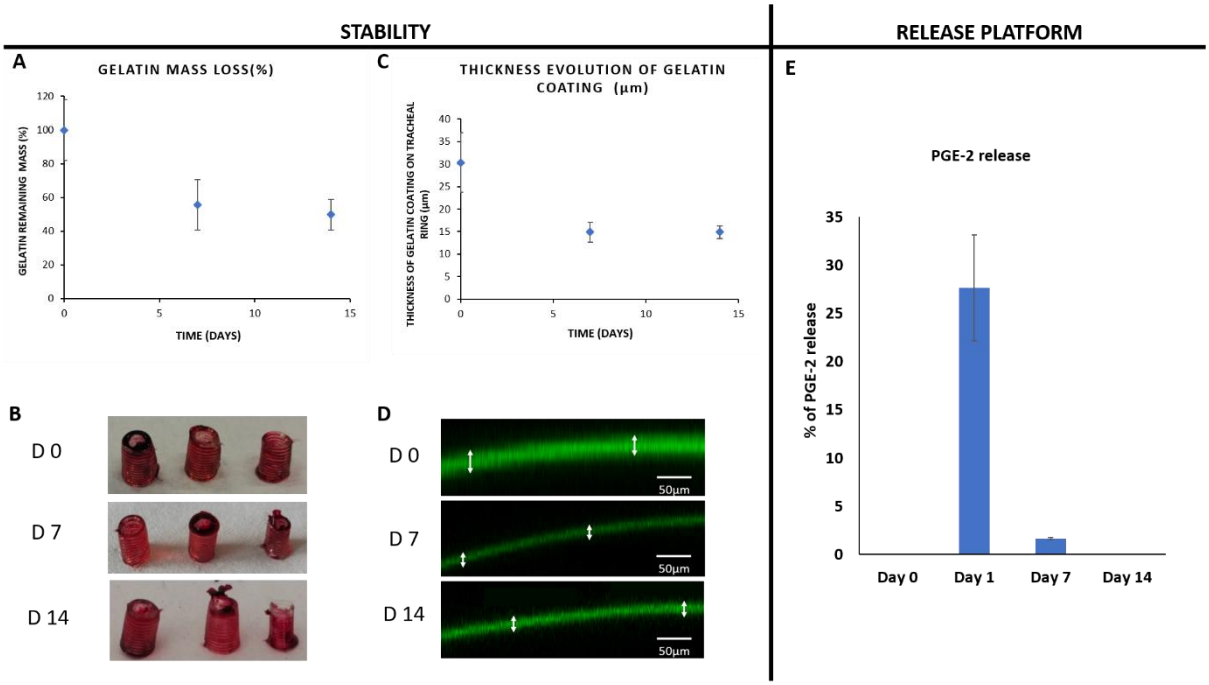

Figure 6. Stability of gelatin coating on 3D printed silicone tracheal patch (A-D) and release properties of the resulting tracheal patch (E). A) Mass loss gelatin coating on top of 3d printed silicone tracheal patch at different time points (Days 0, 7 and 14) of immersion in cell culture medium at 37°C using

Sirius Red/Fast Green collagen staining kit and B) resulting visual aspects of the patch (n=3). C) Determination of the thickness of the gelatin coating on tracheal patch with confocal microscope at different time points (Days 0, 7 and 14) using fluorescently labeled gelatin (Gelatin-FITC) and D) resulting confocal images (n=3). E) Release profile determined by Elisa test for PGE-2 over 14 days in PBS at 37°C. For each release experiment, fresh supernatant was added after each record. For all experiments, values are expressed as mean +/- SD n=3.

3.5 *In vivo* and histology

The reasons for tracheal resection and reconstruction are various ranging from tracheal stenosis to tumors and tracheoesophageal fistula. When the use of biomaterials is necessary, the potential related problems are granulation tissue formation, wound infection and edema. The granulation tissue can be formed within days or within weeks and would require interventions with laser for its removal or if it is too extensive additional stenting of the airways should be performed in order to keep them open. Granulation tissue is supposed to be a temporary formation within the wound dominated by macrophages and neutrophils. Its persistence around implants indicates problems in the resolution of inflammation and healing. Silicone, a non-degradable, hydrophobic polymer, has a certain level of bio-inertness and on average do not induce a strong immune reaction. This has driven its use in many different implantable device scenarios from esophageal stents to breast implants. However, it is common for silicone implants to induce granulomas as the long-term interaction of innate immunity components without the removal of the silicone results in a chronic inflammatory condition which is conducive to granuloma formation [19, 59].

In this study, 3D printed silicone tracheal patches have been produced to repair tracheal defect induced on rats. An incision equivalent to the ablation of two tracheal rings was made on each rat to mimic a defect and then the 3D printed silicone patch was applied to close this opening. Then the in vivo experiment was carried out for 21 days to assess the tissue regeneration around the patch and the influence of the coating on the inflammation and healing process.

Three conditions were performed: i) tracheal silicone patch without any coating **(PDMS)**, ii) tracheal patch coated with gelatin-based hydrogel **(Gel)** and iii) tracheal patch coated with gelatin-based hydrogel loaded with M2Ct2 anti-inflammatory cocktail **(M2Ct2).** The main objective was to evaluate the effect of the anti-inflammatory cocktail on the overall inflammation and integration after implantation. The first parameters checked for this experiment was the survival rate of the animals and 21 days after implantation it was at 33% (2/6 animals) for the first condition **(PDMS)**, 75% (6/8 animals) for the second condition **(Gel)** and 100% (8/8 animals) for the third condition **(M2Ct2: immunomodulatory hydrogel)** (Figure S5A). The main causes of premature death were dyspnea and suffocation in the aftermath of an obstruction in the respiratory tract. Thus the gelatin hydrogel coating by itself seems to have improved the survival rate from 33% to 75% and the use of M2Ct2 cocktail could have an additional effect since it increased the survival rate to 100%. A more biomimicking interface between the implant and the surrounding microenvironment can improve tissue adhesion, prevent dispnea and promote implant integration. However, to confirm these first results, more data about inflammation and tissue integration should be given. Thus, we assessed the systemic level of key pro-inflammatory cytokines in the blood: CCL-2/MCP-1, TNF-alpha, IL-1 beta, CXCL1/KV, IFN gamma and IL-1 alpha (Figure 7). It was statistically not possible to compare the second and third conditions with the first one since only 2 animals survived for 21 days so we only compared the hydrogel vs immunomodulatory hydrogel conditions. After one week of implantation, we observed that four pro-inflammatory cytokines (CXCL1/KV, CCL2/MCP-1, TNF-alpha and IFN gamma) showed a significant decrease in expression in the immunomodulatory hydrogel condition. Then after 21 days, also four cytokines (IL-1 beta, IL-1 alpha, CXCL1/KV, CCL2/MCP-1) showed significant decrease in the immunomodulatory hydrogel condition. The addition of the M2Ct2 cocktail in the gel formulation has a significant effect on the resolution of inflammation since it downregulated the expression of key pro-inflammatory cytokines. Thus this demonstrates that silicone implants can be modified in an easy way to moderate the in vivo inflammation related to the implantation of this material.

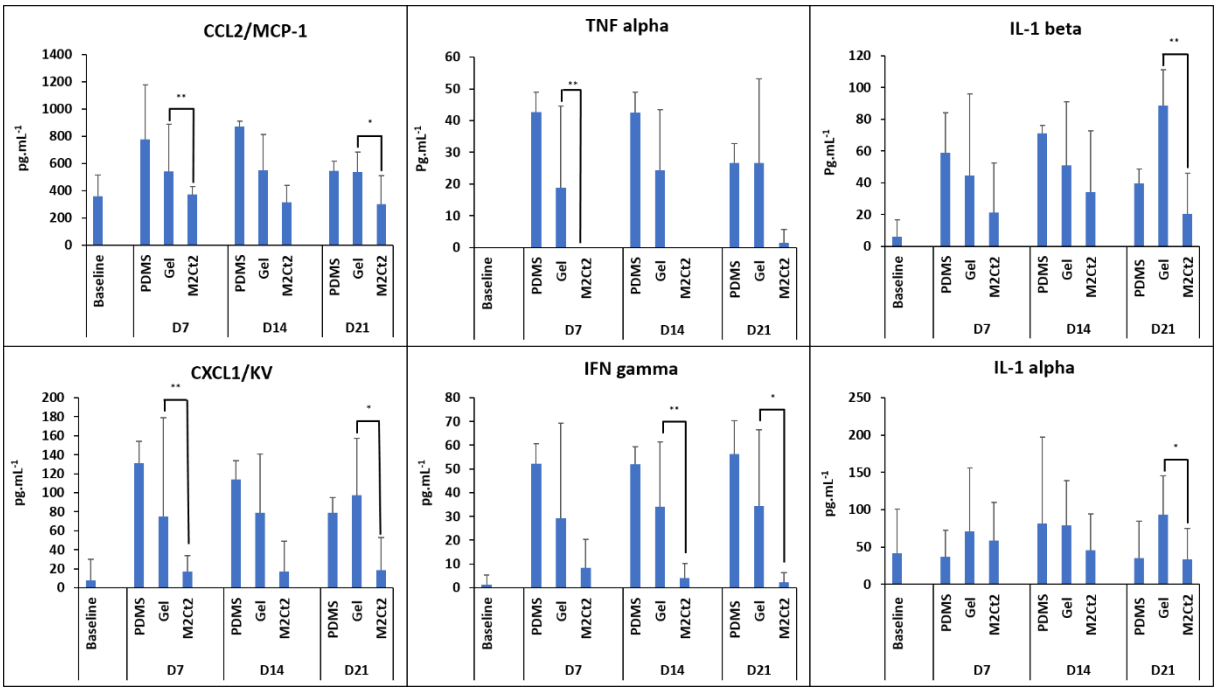

Figure 7. Quantification of 6 (CCL-2/MCP-1, CXCL1/KV, TNF alpha, IFN gamma, IL-1 beta and IL-1 alpha) pro-inflammatory cytokines in the blood serum at different time points of *in vivo* experiment (Days 7, 14, 21). for each condition tested i) silicone (PDMS), ii) silicone + hydrogel (Gel) and iii) silicone + hydrogel + M2Ct2 (M2Ct2: immunomodulatory hydrogel) (n=8). Values are expressed as mean +/- SD n=8, *p<0.05, **p<0.01.

Histology analyses were realized and H&E stainings were performed (Figure 9). To compare the different conditions, the following parameters were considered: chronic (lymphocytes and plasma cells) and acute (neutrophils) inflammatory infiltrate periprosthetic fibrinoid deposition, fibroblastic reaction, edema, periprosthetic histiocytic barrier, tracheal ulceration - the thickness of internal inflammation integrating these parameters (Figure S5B). In the case of silicone based implant without any coating (1st condition), the intensity of both chronic and acute inflammation was high for most of the animals with fibrinoid deposition, edema, and high fibroblastic reaction. The thickness of internal inflammation (between outer part of the implant and the surrounding tissue) was found very important, it reached sometimes 3.2 mm. With this condition, we can see that the level of inflammation was elevated, and it explains the low survival rate. After the deposition of the hydrogel

coating (2nd condition,Gel) at the surface of the implant, most the parameters were downregulated, in particular the thickness of internal inflammation (from 3.2 mm without coating to 0.1 mm with the immunomodulatory coating). The loading of M2Ct2 cocktail in the hydrogel (3rd condition, M2Ct2) shows histology results pretty close to the second condition. There was a slight decrease of chronic and acute inflammation, edema, with a slight overall diminution of the thickness of internal inflammation.

Within the timeframe of the experiments, we did not observe a fully developed granuloma, the extensive presence of immune cells in the form of a granulation tissue was evident when there was no hydrogel interface (Figure 9A, D). The presence of the hydrogel attenuated the reaction as the gelatin hydrogel provides a degradable environment for the incoming immune cells, thus, regulating the initial reaction (Figure 9B, E). However, in order to have a potent effect, the presence of cytokines is essential as a tissue structure more similar to the native epithelium tissue was observed in the conditions where the implants were coated with hydrogels containing the cytokine cocktail (Figure 9C, F). Here, the gels not only provide a suitable substrate for the incoming cells, but they also provide in a controlled manner biochemical signals that would regulate their polarization state.

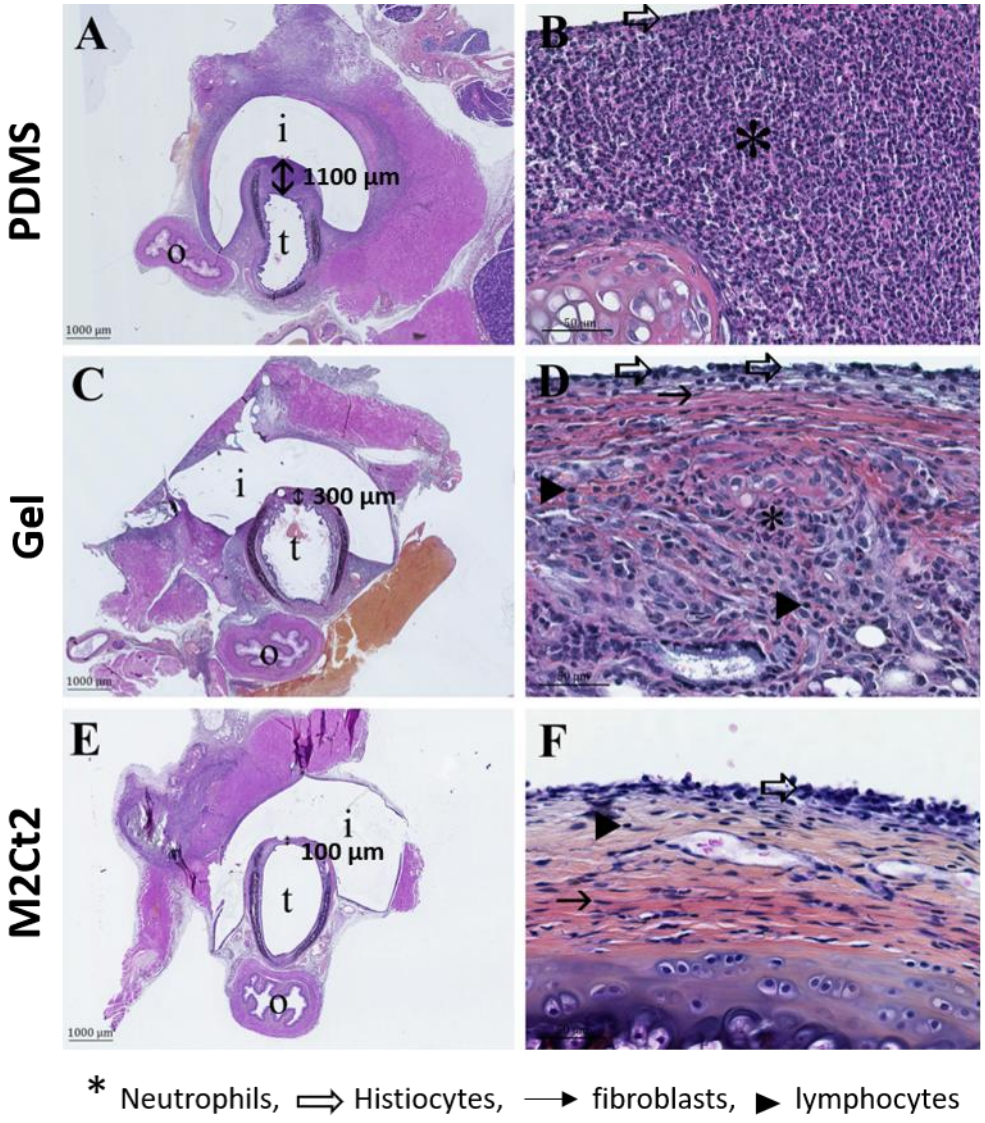

Figure 9: Histological H&E stainings after 21 days of implantation of 3D printed silicone tracheal patch in a rat model. Group 1 (**A,B: PDMS**) shows a marked acute inflammatory response to the implant (i) with numerous neutrophils (*). Group 2 (**C, D: Gel**) shows a moderate chronic and subacute inflammatory response to the implant (i) with lymphocytes (>) associated to few fibroblasts (black arrow) and neutrophils (*). Group 3 (**E, F: M2Ct2: immunomodulatory hydrogel**) shows a slight chronic inflammatory response to the implant (i) with few lymphocytes (>) and fibroblasts (black arrow). In all case histiocytes/macrophages (white arrow) are in contact of the implant (i). Intensity of the fibro-inflammatory reaction due to the implant was evaluated in particular by measuring the thickness between implant (i) and tracheal lumen (t).

Conclusion

Thin ECM-like coatings containing specific immunomodulatory coatings can be used to control the interaction of the non-degradable implant materials with the surrounding tissues. Herein, we demonstrated that a M2 macrophage phenotype inducing cocktail which also prevents MMP secretion can keep the pro-inflammatory cytokine release low and induce M2 macrophage polarization in both 2D and 3D conditions. This cocktail can be loaded in thin gelatin hydrogel and can be slowly released to create an interface which is less conducive to chronic inflammation and has anti-inflammatory effects both locally and at systemic level. Such combination of controlled interfaces can be used to improve the outcomes of implantations via aiding the resolution of inflammation and promoting integration. This immunomodulation strategy is of first interest in the field of tracheal engineering. Indeed, the trachea is essential for respiration thus, if it narrows or collapses, it is life-threatening. The majority of *in vivo* studies conducted on tracheal replacements require the placement of a stent to avoid stenosis due to light infiltration by granular and inflammatory tissue. This requires general anesthesia for stent removal and tolerance problems. Endoluminal stents have shown severe complications (migration, granulation tissue, and biofilm-induced blockages) [60]. In our study, after the deposition of the immunomodulatory coating, we decreased significantly the internal inflammation with an endotracheal lumen that remains wide and allows normal breathing without the use of stents. This coating can be used as a replacement for trachea in new materials.

Acknowledgements:

This project has received funding from the European Union's Seventh Framework Programme for research, technological development and demonstration under grant agreement no. 602694 (IMMODGEL), from the European Union's Horizon 2020 research and innovation programme under grant agreement No 760921(PANBioRA). This work was supported by the French government trough FASSIL project, selected by FUI (Fonds Unique Interministériel). We would like to thank Manon Farcé

(Pôle Technologique du CRCT - Plateau de Cytométrie – INSERM UMR1037) for her technical assistance with flow cytometry and Karim Benmlih for the design and the fabrication of the specific holders to coat gelatin hydrogel on the tracheal patch

Conflicts of interest

"There are no conflicts to declare".

Authors contributions

J. Barthes: Conceptualization, Methodology, Data analysis, Writing-Original draft preparation, Reviewing, Editing.

P. Lagarrigue: Data analysis, methodology, Investigation, Experimental work (in vivo experiment, material characterization, Reviewing.

V. Ryabov: Data analysis, Experimental work (RTq-PCR experiment, cytokines analyses).

G. Lutzweiler: Experimental work (contact angle measurement).

J. Michel: Experimental work (3D cell encapsulation experiment).

C. Muller: Experimental work (material preparation and characterization).

E.-J. Courtial: Data analysis, Experimental work (3D printing, rheology and surface characterization), Writing-Original draft preparation, Reviewing.

C. Marquette: Conceptualization, Methodology, Reviewing.

F. Projetti: Data analysis, Experimental work (Histology stainings).

J. Kzhyskowska : Conceptualization, Reviewing.

P. Lavalle : Conceptualization, Methodology, Writing-Original draft preparation, Reviewing

N.E.Vrana: Conceptualization, Methodology, Investigation, Data analysis, Writing-Original draft preparation, Reviewing.

A. Dupret-Bories: Conceptualization, Methodology, Data analysis, Experimental work (in vivo experiment), Writing-Original draft preparation, Reviewing.

References

1. Auchincloss, H.G. and C.D. Wright, *Complications after tracheal resection and reconstruction: prevention and treatment.* Journal of thoracic disease, 2016. **8**(Suppl 2): p. S160-S167.
2. Rosen, F.S., A.M. Pou, and W.L. Buford, *Tracheal Resection with Primary Anastomosis in Cadavers: The Effects of Releasing Maneuvers and Length of Tracheal Resection on Tension.* Annals of Otology, Rhinology & Laryngology, 2003. **112**(10): p. 869-876.
3. Grillo, H.C., *Tracheal replacement: a critical review.* The Annals of Thoracic Surgery, 2002. **73**(6): p. 1995-2004.
4. Virk, J.S., et al., *Prosthetic reconstruction of the trachea: A historical perspective.* World journal of clinical cases, 2017. **5**(4): p. 128-133.
5. Delaere, P.R., Z. Liu, and R. Hermans, *Laryngotracheal Reconstruction With Tracheal Patch Allografts.* The Laryngoscope, 1998. **108**(2): p. 273-279.
6. Kim, D.Y., et al., *Tissue-engineered allograft tracheal cartilage using fibrin/hyaluronan composite gel and its in vivo implantation.* The Laryngoscope, 2010. **120**(1): p. 30-38.
7. Shigemitsu, K., et al., *A Case of Thyroid Cancer Involving the Trachea: Treatment by Partial Tracheal Resection and Repair with a Latissimus Dorsi Musculocutaneous Flap.* Japanese Journal of Clinical Oncology, 2000. **30**(5): p. 235-238.
8. Lee, J.H., et al., *Triple-layered polyurethane prosthesis with wrinkles for repairing partial tracheal defects.* The Laryngoscope, 2014. **124**(12): p. 2757-2763.
9. Choi, H., Suh, H., Lee, JH., Park, SN., Shin, SH., Kim, YH., Chung, SM., Kim, HK., Lim, JY., Kim, HS., *A polyethylene glycol grafted bi-layered polyurethane scaffold: preliminary study of a new candidate prosthesis for repair of a partial tracheal defect.* European Archives of Oto-Rhino-LAryngology, 2008. **265**(7): p. 809-816.
10. Cull, D.L., et al., *Tracheal reconstruction with polytetrafluoroethylene graft in dogs.* The Annals of Thoracic Surgery, 1990. **50**(6): p. 899-901.
11. Ghorbani, F., et al., *In-vivo characterization of a 3D hybrid scaffold based on PCL/decellularized aorta for tracheal tissue engineering.* Materials Science and Engineering: C, 2017. **81**: p. 74-83.
12. Soo Yeon, J., et al., *3D printed polyurethane prosthesis for partial tracheal reconstruction: a pilot animal study.* Biofabrication, 2016. **8**(4): p. 045015.
13. Chang, J.W., et al., *Tissue-Engineered Tracheal Reconstruction Using Three-Dimensionally Printed Artificial Tracheal Graft: Preliminary Report.* Artificial Organs, 2014. **38**(6): p. E95-E105.
14. Yamashita, M., et al., *Tracheal Regeneration After Partial Resection: A Tissue Engineering Approach.* The Laryngoscope, 2007. **117**(3): p. 497-502.
15. Friedman, M. and A.D. Mayer, *Laryngotracheal Reconstruction in Adults with the Sternocleidomastoid Myoperiosteal Flap.* Annals of Otology, Rhinology & Laryngology, 1992. **101**(11): p. 897-908.
16. Abdülcemal Işik, U., et al., *Prosthetic reconstruction of the trachea in rabbit.* The Journal of cardiovascular surgery, 2002. **43**(2): p. 281-286.
17. Propst, E.J., et al., *Pediatric tracheal reconstruction using cadaveric homograft.* Archives of Otolaryngology–Head & Neck Surgery, 2011. **137**(6): p. 583-590.

18. Anderson, J.M., A. Rodriguez, and D.T. Chang, *Foreign body reaction to biomaterials.* Seminars in Immunology, 2008. **20**(2): p. 86-100.
19. Jham, B.C., et al., *Granulomatous Foreign-Body Reaction Involving Oral and Perioral Tissues After Injection of Biomaterials: A Series of 7 Cases and Review of the Literature.* Journal of Oral and Maxillofacial Surgery, 2009. **67**(2): p. 280-285.
20. Kzhyshkowska, J., et al., *Macrophage responses to implants: prospects for personalized medicine.* Journal of Leukocyte Biology, 2015. **98**(6): p. 953-962.
21. Al-Maawi, S., et al., *In vivo Implantation of a Bovine-Derived Collagen Membrane Leads to Changes in the Physiological Cellular Pattern of Wound Healing by the Induction of Multinucleated Giant Cells: An Adverse Reaction?* Frontiers in Bioengineering and Biotechnology, 2018. **6**(104).
22. Vishwakarma, A., et al., *Engineering Immunomodulatory Biomaterials To Tune the Inflammatory Response.* Trends in Biotechnology, 2016. **34**(6): p. 470-482.
23. Hotaling, N.A., et al., *Biomaterial Strategies for Immunomodulation.* Annual Review of Biomedical Engineering, 2015. **17**(1): p. 317-349.
24. Gordon, S., *Alternative activation of macrophages.* Nature Reviews Immunology, 2003. **3**: p. 23.
25. Spiller, K.L., et al., *The role of macrophage phenotype in vascularization of tissue engineering scaffolds.* Biomaterials, 2014. **35**(15): p. 4477-4488.
26. Dollinger, C., et al., *Incorporation of resident macrophages in engineered tissues: Multiple cell type response to microenvironment controlled macrophage-laden gelatine hydrogels.* Journal of Tissue Engineering and Regenerative Medicine, 2018. **12**(2): p. 330-340.
27. Dziki, J.L. and S.F. Badylak, *Immunomodulatory biomaterials.* Current Opinion in Biomedical Engineering, 2018. **6**: p. 51-57.
28. Rostam, H.M., et al., *The impact of surface chemistry modification on macrophage polarisation.* Immunobiology, 2016. **221**(11): p. 1237-1246.
29. Singh, S., et al., *Unbiased Analysis of the Impact of Micropatterned Biomaterials on Macrophage Behavior Provides Insights beyond Predefined Polarization States.* ACS Biomaterials Science & Engineering, 2017. **3**(6): p. 969-978.
30. Dollinger, C., et al., *Controlling Incoming Macrophages to Implants: Responsiveness of Macrophages to Gelatin Micropatterns under M1/M2 Phenotype Defining Biochemical Stimulations.* Advanced Biosystems, 2017. **1**(6): p. 1700041.
31. Vasconcelos, D.P., et al., *Development of an immunomodulatory biomaterial: Using resolvin D1 to modulate inflammation.* Biomaterials, 2015. **53**: p. 566-573.
32. Minardi, S., et al., *IL-4 Release from a Biomimetic Scaffold for the Temporally Controlled Modulation of Macrophage Response.* Annals of Biomedical Engineering, 2016. **44**(6): p. 2008-2019.
33. Riabov, V., et al., *Generation of anti-inflammatory macrophages for implants and regenerative medicine using self-standing release systems with a phenotype-fixing cytokine cocktail formulation.* Acta Biomaterialia, 2017. **53**: p. 389-398.
34. Drury, J.L. and D.J. Mooney, *Hydrogels for tissue engineering: scaffold design variables and applications.* Biomaterials, 2003. **24**(24): p. 4337-4351.
35. Chaudhuri, O., et al., *Hydrogels with tunable stress relaxation regulate stem cell fate and activity.* Nature Materials, 2015. **15**: p. 326.
36. Sirousazar, M., Forough, M., Farhadi, K., Shaabani, Y., Molaei, R., *Hydrogels: Properties, Preparation, Characterization and Biomedical, Applications in Tissue Engineering, Drug, Delivery and Wound Care*, in *Advanced Healthcare Materials*, Wiley, Editor. 2014.
37. Knopf-Marques, H., et al., *Immunomodulation with Self-Crosslinked Polyelectrolyte Multilayer-Based Coatings.* Biomacromolecules, 2016. **17**(6): p. 2189-2198.
38. Barthes, J., et al., *Priming cells for their final destination: microenvironment controlled cell culture by a modular ECM-mimicking feeder film.* Biomaterials Science, 2015. **3**(9): p. 1302-1311.

39. Özçelik, H., et al., *Harnessing the Multifunctionality in Nature: A Bioactive Agent Release System with Self-Antimicrobial and Immunomodulatory Properties.* Advanced Healthcare Materials, 2015. **4**(13): p. 2026-2036.
40. Knopf-Marques, H., et al., *Auxiliary Biomembranes as a Directional Delivery System To Control Biological Events in Cell-Laden Tissue-Engineering Scaffolds.* ACS Omega, 2017. **2**(3): p. 918-929.
41. Jorge, R.G., et al., *Experimental study of a new porous tracheal prosthesis.* The Annals of Thoracic Surgery, 1990. **50**(2): p. 281-287.
42. Dumon, J.-F., et al., *Seven-year experience with the Dumon prosthesis.* Journal of Bronchology, 1996. **3**: p. 6-10.
43. Montgomery, W.W., *Silicone Tracheal T-Tube.* Annals of Otology, Rhinology & Laryngology, 1974. **83**(1): p. 71-75.
44. Gao, M., et al., *Tissue-engineered trachea from a 3D-printed scaffold enhances whole-segment tracheal repair.* Scientific Reports, 2017. **7**(1): p. 5246.
45. Courtial, E.-J., et al., *Silicone rheological behavior modification for 3D printing: Evaluation of yield stress impact on printed object properties.* Additive Manufacturing, 2019. **28**: p. 50-57.
46. Vergnon, J.-M., F. Costes, and J.-C. Polio, *Efficacy and Tolerance of a New Silicone Stent for the Treatment of Benign Tracheal Stenosis: Preliminary Results.* Chest, 2000. **118**(2): p. 422-426.
47. Puma, F., et al., *Long-term safety and tolerance of silicone and self-expandable airway stents: an experimental study.* The Annals of Thoracic Surgery, 2000. **69**(4): p. 1030-1034.
48. Gratchev, A., et al., *Interleukin-4 and Dexamethasone Counterregulate Extracellular Matrix Remodelling and Phagocytosis in Type-2 Macrophages.* Scandinavian Journal of Immunology, 2005. **61**(1): p. 10-17.
49. Barthes, J., et al., *Immune Assisted Tissue Engineering via Incorporation of Macrophages in Cell-Laden Hydrogels Under Cytokine Stimulation.* Frontiers in bioengineering and biotechnology, 2018. **6**: p. 108-108.
50. Kzhyshkowska, J., et al., *Alternatively Activated Macrophages Regulate Extracellular Levels of the Hormone Placental Lactogen via Receptor-Mediated Uptake and Transcytosis.* The Journal of Immunology, 2008. **180**(5): p. 3028.
51. Kwon, D., et al., *Extra-Large Pore Mesoporous Silica Nanoparticles for Directing in Vivo M2 Macrophage Polarization by Delivering IL-4.* Nano Letters, 2017. **17**(5): p. 2747-2756.
52. Kivelä-Rajamäki, M., et al., *Levels and molecular forms of MMP-7 (matrilysin-1) and MMP-8 (collagenase-2) in diseased human peri-implant sulcular fluid.* Journal of Periodontal Research, 2003. **38**(6): p. 583-590.
53. Tang, T., et al., *Macrophage responses to lipopolysaccharide are modulated by a feedback loop involving prostaglandin E2, dual specificity phosphatase 1 and tristetraprolin.* Scientific Reports, 2017. **7**(1): p. 4350.
54. Gill, S.K., et al., *The anti-inflammatory effects of PGE2 on human lung macrophages are mediated by the EP4 receptor.* British Journal of Pharmacology, 2016. **173**(21): p. 3099-3109.
55. MacKenzie, K.F., et al., *PGE₂ Induces Macrophage IL-10 Production and a Regulatory-like Phenotype via a Protein Kinase A–SIK–CRTC3 Pathway.* The Journal of Immunology, 2013. **190**(2): p. 565.
56. Cha, B.-H., et al., *Integrin-Mediated Interactions Control Macrophage Polarization in 3D Hydrogels.* Advanced Healthcare Materials, 2017. **6**(21): p. 1700289.
57. Kzhyshkowska, J., A. Gratchev, and S. Goerdt, *Stabilin-1, a homeostatic scavenger receptor with multiple functions.* Journal of Cellular and Molecular Medicine, 2006. **10**(3): p. 635-649.
58. Rantakari, P., et al., *Stabilin-1 expression defines a subset of macrophages that mediate tissue homeostasis and prevent fibrosis in chronic liver injury.* Proceedings of the National Academy of Sciences, 2016. **113**(33): p. 9298-9303.
59. Steinbach, B.G., et al., *Breast implants, common complications, and concurrent breast disease.* RadioGraphics, 1993. **13**(1): p. 95-118.

60. Gorostidi, F., et al., *Extraluminal biodegradable splint to treat upper airway anterior malacia: A preclinical proof of principle.* The Laryngoscope, 2018. **128**(2): p. E53-E58.